

SPIRE Science Verification Review

RAL

January 26, 27 2006

Bolometer Array Noise Performance in PFM1 and PFM2 Test Campaigns

Document Number: SPIRE-JPL-REP-002570

Issue 1.0

16 January 2006

**Bernhard Schulz (IPAC)
with contributions from Kevin Xu and Lijun Zhang**

Contents

1.	Introduction and scope.....	2
2.	The data.....	2
3.	Broken or missing channels.....	3
4.	Basic noise.....	3
5.	Spectral features.....	4
6.	Noise due to temperature instabilities.....	4
7.	Spontaneous spiking.....	4
8.	Influence of bias frequency.....	5
9.	Summary and conclusions.....	5
10.	Annex: Figures of noise levels during night runs.....	6

1. Introduction and scope

This note gives a brief overview of the noise performance of the PFM photometer and spectrometer detectors during the PFM1 and PFM2 tests respectively. The emphasis is on the derivation of the noise of the undisturbed detectors, hereafter called basic noise. We also make an assessment of the functionality of detector channels as far as measured, and discuss particular noise phenomena.

Analysis of data with LIA boards at different positions, which were obtained towards the end of the PFM2 campaign, as well as the noise analysis of spectrometer data from the PFM2 campaign, are not covered in this report.

2. The data

Data were retrieved from databases PFM1_test2 for the spectrometer arrays and PFM2_test1 for the photometer arrays. The data were taken during the night with minimal optical loading, with the instrument on and the data acquisition system running. This way we expect a minimum of environmental disturbances. The data timelines divided into 30 min blocks and saved into FITS files.

For the SSW and SLW arrays, three nights were considered, starting respectively on 2005-Mar-04 22:17, 2005-Mar-09 00:22, 2005-Mar-09 22:40 and extending over 5 to 6 hours.

For the PSW, PMW, and PLW arrays, four nights were considered, starting respectively on 2005-Sep-08 22:12, on 2005-Sep-12 21:54, on 2005-Sep-14 23:17, on 2005-Sep-27 21:32, and extending over 7, 9, 7, and 9 hours respectively.

The data time tags contain errors that were automatically corrected. For the correction it was assumed that the majority of time tags are correct in absolute terms and that data are appearing in the correct order. Time tags were corrected such that the average data rate was kept. Two time errors were observed: one shows a sudden offset in time for a number of readouts, which reverts back after a while; the second shows short gaps of up to a few seconds of duration, in an otherwise regular sequence of data. For this analysis the first error was corrected by generating new time tags that are in sequence, the second error was corrected by shifting the entire remaining sequence back to remove the gap.

3. Broken or missing channels

In the following the detector channels are designated by either their QLA channel number in FULL mode, or by their JPL detector names. The prefixes PS, PM, PL, SS, SL identify the detector array.

The PFM1 tests with only the spectrometer detectors had all channels connected. However due to a harness problem, the shielding of a connector was compromised. The corresponding channel range 25-48 therefore exhibits excess noise, of which channels 25-42 are connected to detector pixels.

Due to the lack of some LIA boards during the PFM2 tests, the following photometer channel ranges were not available: 1-32, 129-160, 225-256. In addition the connector J31 of the photometer JFET module HSJFP was disconnected. These lines correspond to the PSW BDA connector J1, which corresponds to channels 49-72.

In the following we list a number of channels that were expected to be functional but did not show a signal during instrument tests. For convenience the QLA channel number is given in brackets. In PS_A10(98) all data points display zero. The channel range PS_G5(121) to PS_J7(128) shows no signal similar to other functional detectors. It is suspected that due to insufficient loading the corresponding JFET module did not turn on. Channel PM_G9 (257) does show a very different signal from all other detectors and appears to be disconnected. The thermistor pixel PM_T2(219) shows all data points zero as does pixel PM_B6(276).

On the other hand Channels, PS_F14(83), PS_H16(93) and PS_E9(104) were not measured in BoDAC but are nevertheless functional on instrument level.

SS_D5(29) was reported broken and shows very high noise in PFM1 tests, however it is using one of the badly shielded channels. The dark pixel SL_DK2(67) was reported broken and in the PFM1 tests shows a noise level lower than all other channels of the array.

SS_D6(28) was not measured in BoDAC but shows reasonable noise levels in PFM1.

Due to these circumstances, the only diagnostic pixels left of thermistors (bolometer without spider web), dark pixels and resistor pixels are for PSW one dark pixel, for PLW two dark pixels and one thermistor, and for PMW one dark pixel, one thermistor and one resistor.

4. Basic noise

To measure the white noise level, the power spectra for each pixel and each individual 30-min dataset were calculated. From the power spectrum the white noise level is determined as the median of the 0.5-3.0 Hz interval. As any external disturbance of the system will make the noise level increase, the basic noise level is determined as the minimum for each night and each pixel.

The bias for the PFM1 tests (10.7 mV for SSW and 12.6 mV for SLW) as well as the PFM2 tests (10 mV all arrays) was not the optimum level for minimum detector NEP. Expected noise levels under these different conditions were derived from standard bolometer theory according to Mather, using the JPL measured characteristic bolometer parameters, and actual temperatures. The data for the spectrometer channels from the PFM1 campaign are plotted in the Annex in Figs. 1-3. The data for the photometer channels, except those ranges that were known not to be functional, are shown in Figs. 4-13.

The night with the lowest noise for the spectrometers was the 2005-Mar-09 00:22 run, hereafter called night 2. For the photometers, different nights show lowest levels for different detector arrays and even

connectors. The spectrometer arrays reach average minimum noise levels at about 30% more than the theoretical values. Excluding the compromised second SSW module, and looking for a consistently higher noise level w.r.t. the other channels, relatively more noisy pixels are SS_A3(3), SS_B2(8), SS_F2(20), SL_B2(59), SL_D4(68), SL_C5(69), SL_A3(71). The photometers show an average increase of the noise levels over the theoretical values by rather 10-20%, which is lower than for the spectrometer arrays. However, as grounding issues were also affecting the PFM1 campaign, and lower noise values were found in spectrometer measurements with different bias frequencies, the actual spectrometer noise may also be rather in the 10-20% region. Relatively noisy pixels were found to be PS_H4(40), PS_H13(81), PS_G13(82), PS_G13(82), PS_G14(87), PS_DP2(94), PS_B9 (106).

5. Spectral features

The power spectra display a number of features that sometimes vary from one night to the other. The PSW array found the pixels PS_J2(33), PS_J3(36), PS_J4(41), PS_J5(47), PS_J12(80), PS_J13(85), PS_J14(88), PS_DP2(94), with a broad 5-Hz bump, apparently limited to the J02 and J04 connectors. This feature disappeared during the second and third night and re-appeared during the last night as a sharper microphonic line. The PLW array exhibits a bump centred at 1 Hz for pixels PL_A1(166), PL_D1(173), PL_D3(175), PL_D4(176), PL_C3(178), and PL_DP2(191). The PMW shows several broad features somewhat similar to the 1Hz feature of the PLW in pixels PM_T1(194), PM_B12(195), PM_C13(196), PM_B10(205), and PM_A8(213). Most PMW channels also show a sharp 7-Hz line. The overall picture of these features looks rather inconclusive and may be driven by external influences.

6. Noise due to temperature instabilities

The 1/f knee frequencies in the power spectra were found to be considerably higher than during unit-level testing in the JPL BoDAC facility. This is, however, due to a strongly drifting baseplate temperature, especially during the PFM2 test campaign. This conclusion is drawn from the observation that all functional bolometer signals follow the same drift pattern, while the PMW resistor signal remains stable. Additionally the temperature sensor connected to the cold finger (SUBKTEMP) shows a clear anticorrelation with the signal of the functional bolometers including the available thermistor pixels, although the resolution of its A/D converter is rather limited (see the example in Fig. 13 in the Annex). We further verified with simulated detector data, that a slope in the signal timeline raises the 1/f knee frequency but does not impact the white noise level as long as it can be distinguished. The detector temperature seemed to be more stable during the PFM1 tests.

7. Spontaneous spiking

During the PFM2 campaign we observed at times instantaneous spontaneous spiking of the signal in the PSW signals (See Fig. 14). This was correlated in all functional detector pixels of this array. The PLW and PMW arrays showed some obviously related baseline drift, but only few spikes during the same time. Different types of spikes are observed as seen in Fig. 15, showing signals from exemplary pixels of the PSW, PLW and, PMW arrays and an overplotted smoothed baseline signal (in gray), that most other pixels of the respective detector array are following. All three arrays show a strong thermal spike with a large time constant. In addition the PSW and the PMW show one and two additional spikes respectively with a shorter time constant, which is not seen in the other arrays.

8. Influence of bias frequency

As verified in the PFM1 spectrometer tests, the bias frequency also has an important influence on the noise. Fig. 16 shows the median noise (excluding the noisy second module of SSW) over the spectrometer arrays depending on bias frequency. The lowest noise is found for 106-Hz bias frequency, while encountering a particularly high noise level at 70 Hz. The same assessment still remains to be done for the photometer during the PFM2 test campaign.

9. Summary and conclusions

1. Data from all five SPIRE PFM detector arrays were analyzed regarding detector noise. Data time tags had to be corrected. A number of channels were not functional due to missing LIA boards or due to an open connector. Twelve photometer pixels were not measured in PFM2 due to a JFET not turning on or broken lines. Three photometer pixels, not measured in BoDAC, were confirmed functional in PFM2. Two broken spectrometer pixels show unusual noise levels as expected, while a pixel not measured in BoDAC shows reasonable noise levels. Confirmation using load curve data remains to be done. In particular, due to the unequipped LIA boards, only few diagnostic channels were available.
2. The large majority of spectrometer and photometer signals show only 30% and 10-20% more noise respectively than theoretical expectations from model calculations made for the actual biases that were used. Only seven pixels in the spectrometer and seven pixels in the photometer exhibit greater excess noise. The basic spectrometer noise may even be lower, as a strong dependence on bias frequency was found.
3. The quiet signal is disturbed by variations and instability of the base plate temperature, which were stronger and more erratic for the PFM2 tests. In addition strong spikes were observed, that sometimes appear in series. They show at least two different time constants, and can appear solely on one detector array, or on all three photometer arrays simultaneously.
4. The basic white noise levels look satisfactory and are quite close to the theoretical expectations. It is however important to achieve a better understanding of the thermal instability that affected the system during the PFM2 campaign, where the full complement of detector arrays was integrated for the first time. It will be important to verify in the course of PFM3 testing (which will involve the fully equipped flight DRCU) that these are limitations of the test facility, and do not represent limitations of the instrument systems.

10. Annex: Figures of noise levels during night runs

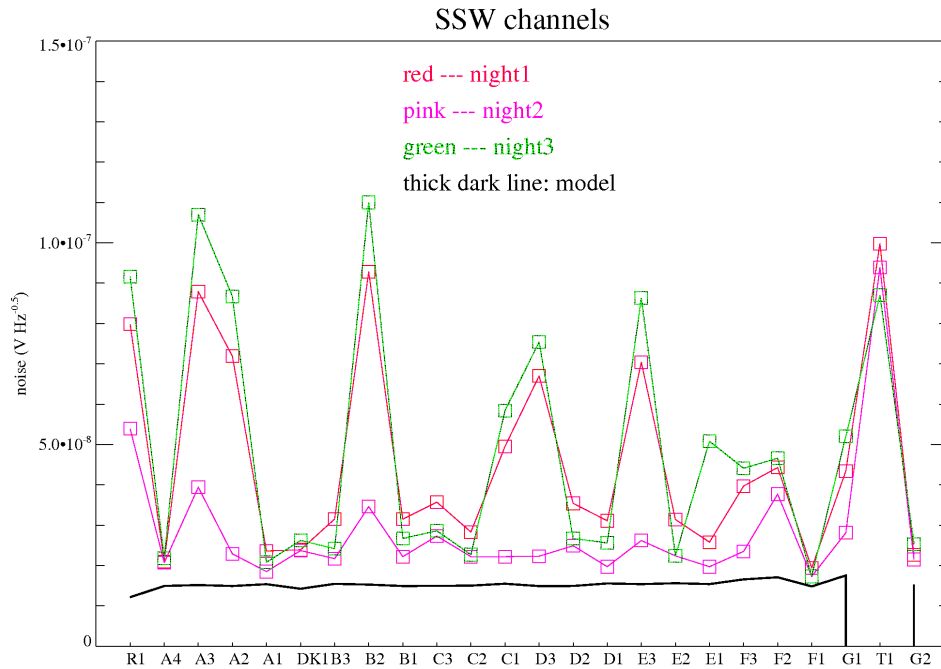


Figure 1: Noise levels of first SSW module during 3 different night runs. The x-axis shows the pixel name. the y-axis shows noise in [V Hz^{-0.5}]. The theoretical noise is shown as a black line.

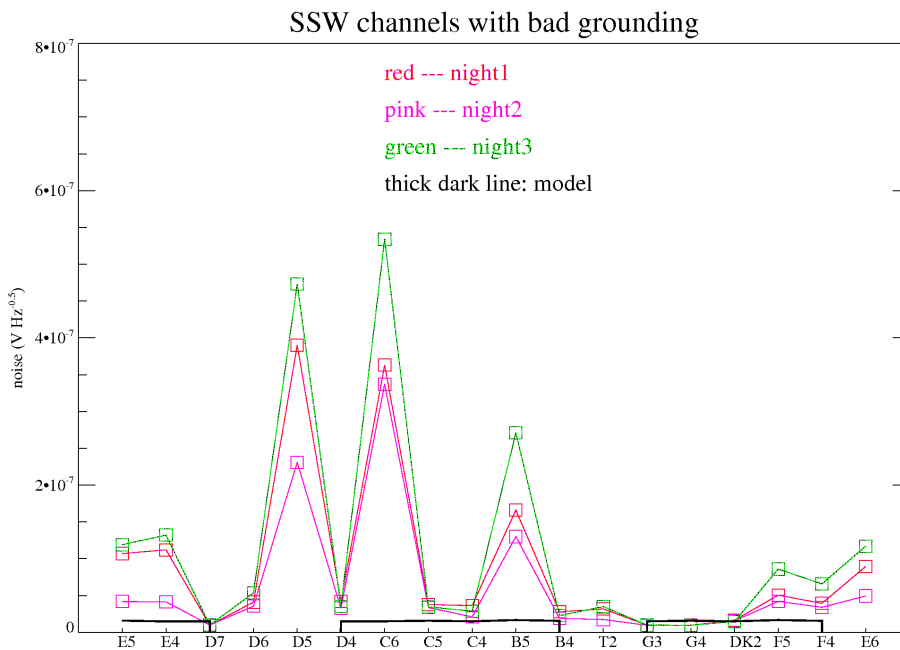


Figure 2: Noise levels of second SSW module during 3 different night runs. This module suffered excess noise due to problems with the shielding.

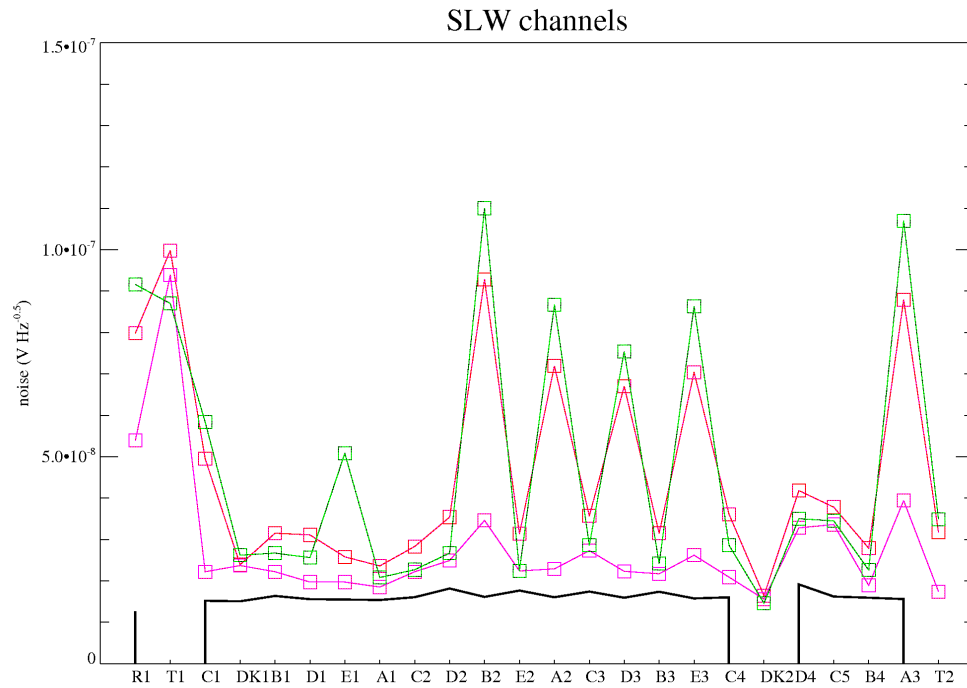


Figure 3: Noise levels of SLW module during 3 different night runs.

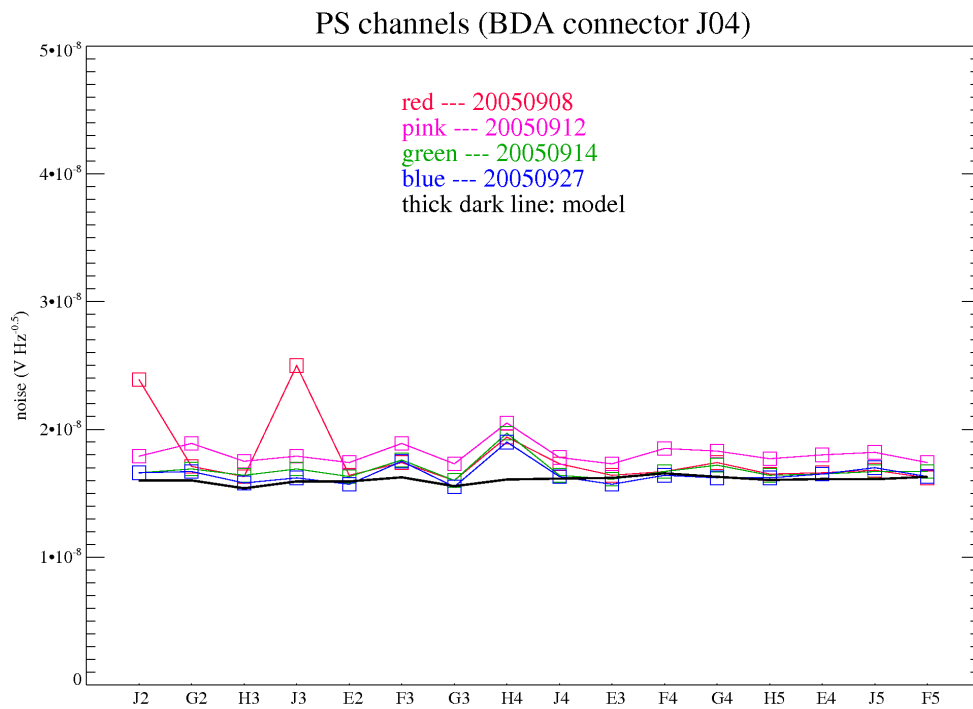


Figure 4: Noise levels of second PSW module during 4 different night runs.

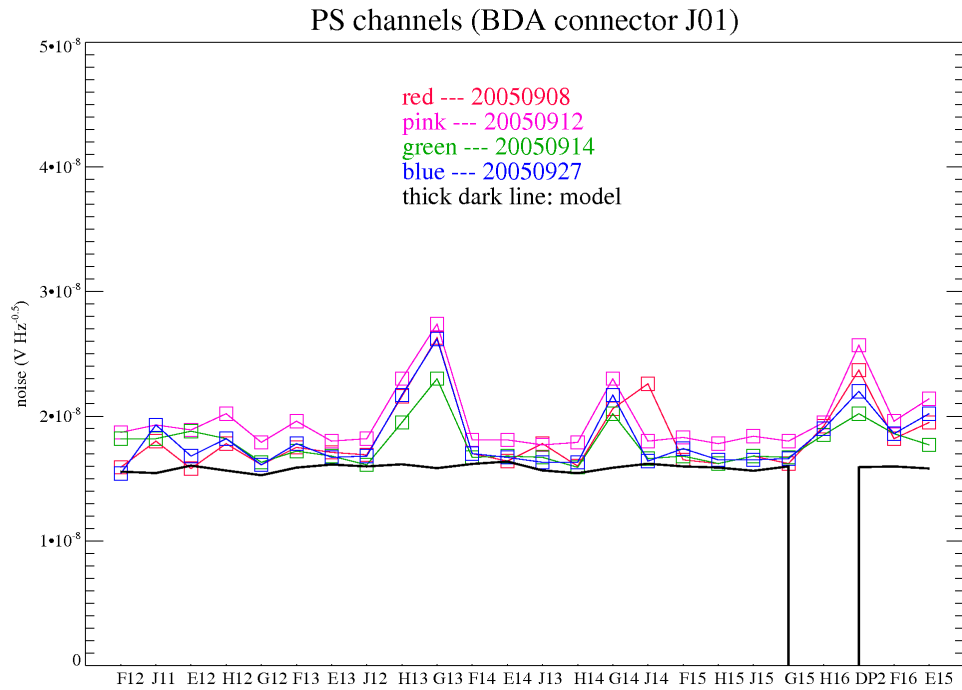


Figure 5: Noise levels of fourth PSW module during 4 different night runs.

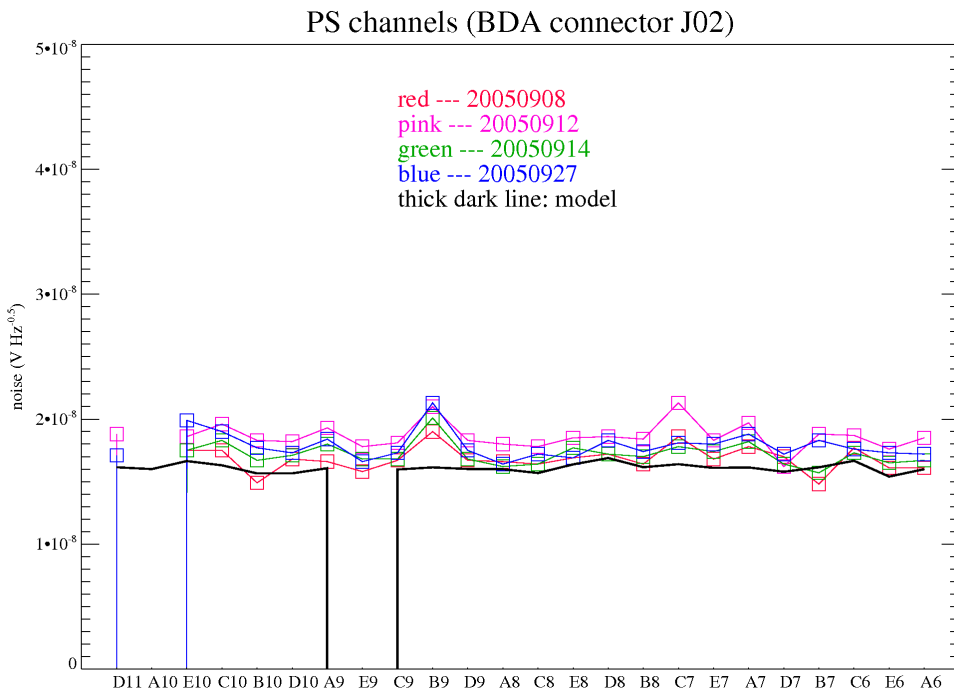


Figure 6: Noise levels of fifth PSW module during 4 different night runs.

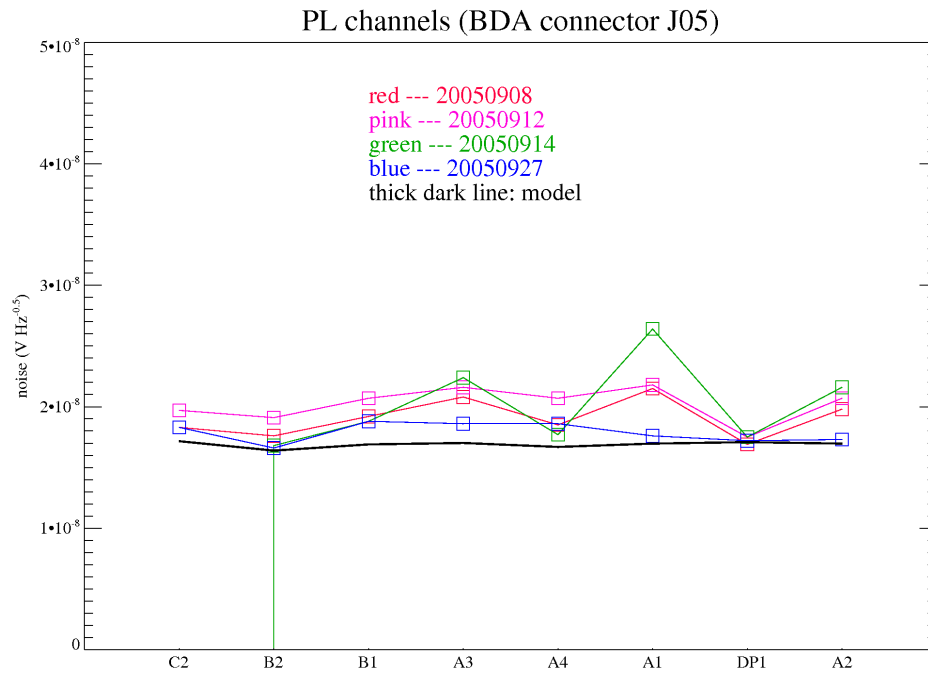


Figure 7: Noise levels of first PLW module during 4 different night runs.

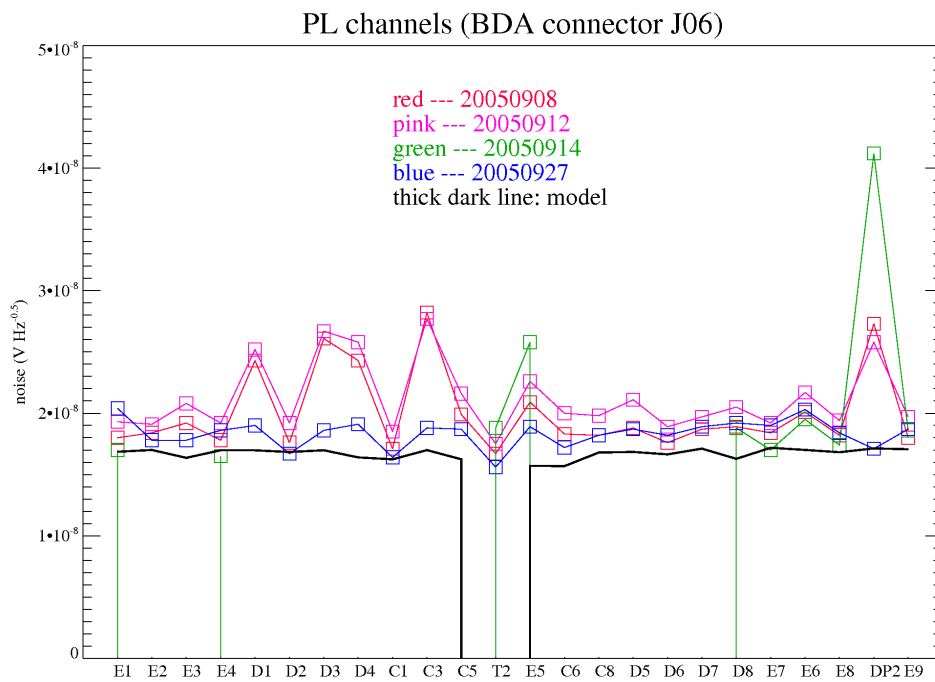


Figure 8: Noise levels of second PLW module during 4 different night runs.

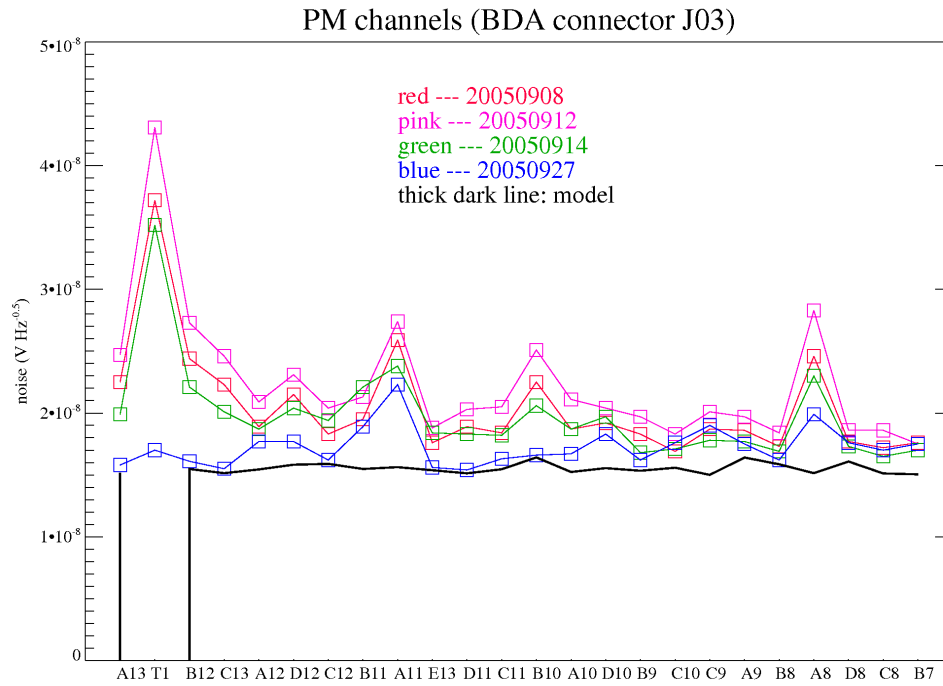


Figure 9: Noise levels of first PMW module during 4 different night runs.

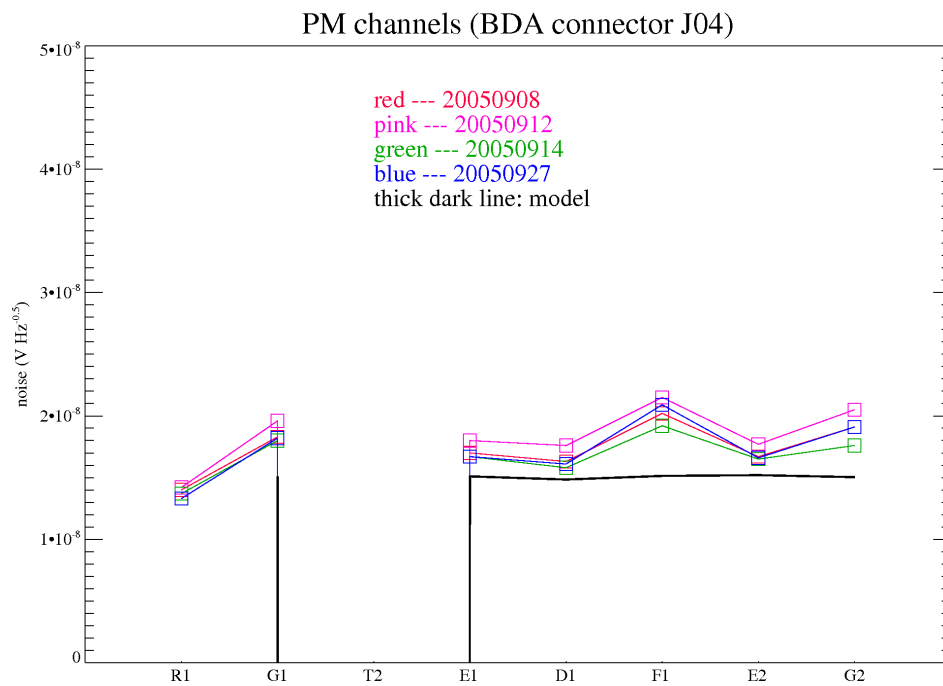


Figure 10: Noise levels of second PMW module during 4 different night runs.

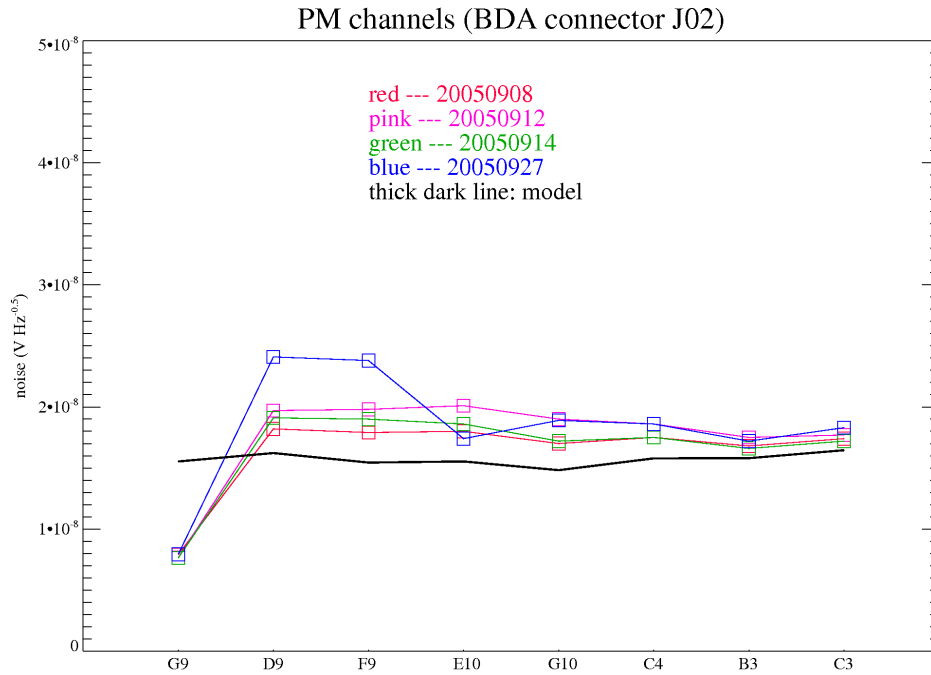


Figure 11: Noise levels of third PMW module during 4 different night runs.

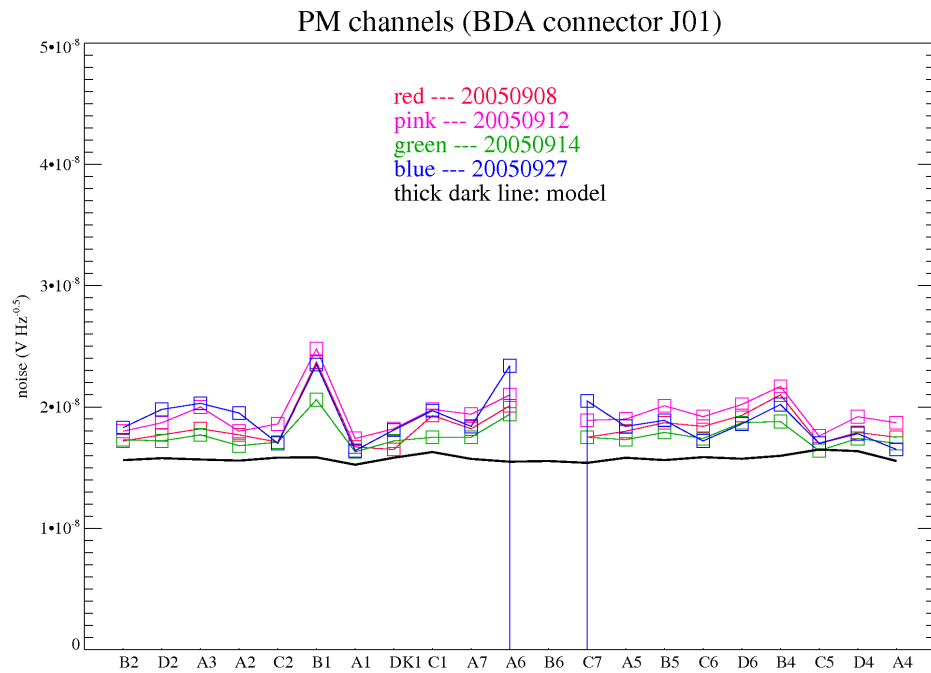


Figure 12: Noise levels of fourth PMW module during 4 different night runs.

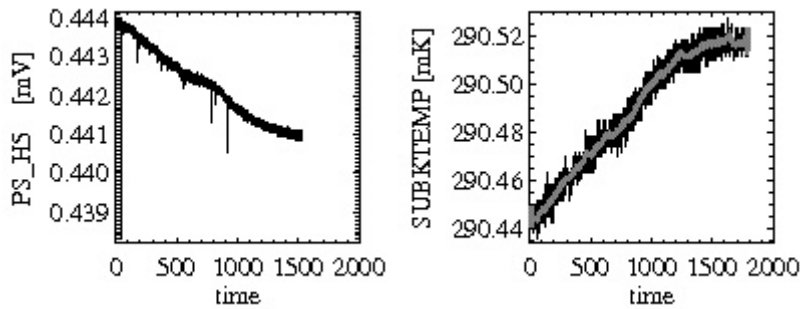


Figure 13: Plots of anticorrelated drifting signals of bolometer detector PS_H5 and the 300mK temperature sensor.

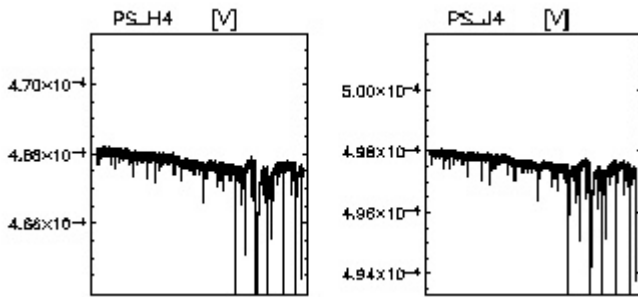


Figure 14: Spontaneous spiking occurring within a 30 min interval.

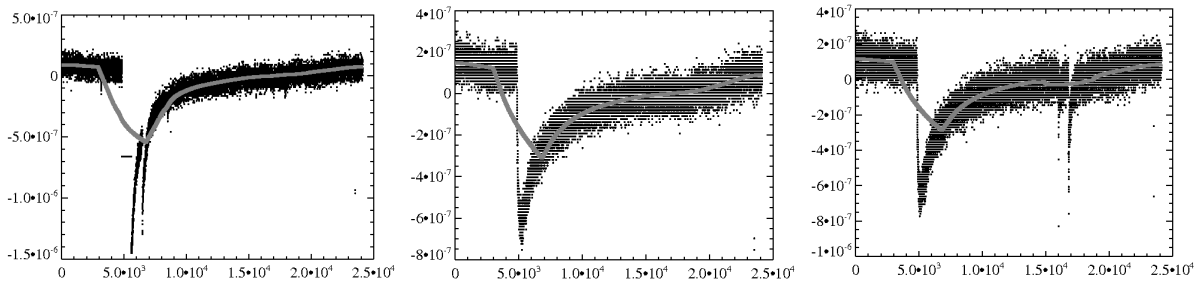


Figure 15: Contemporaneous signal plots versus time of exemplary detector pixels of PSW, PLW and PMW detectors (from left to right). Different spike types can be seen.

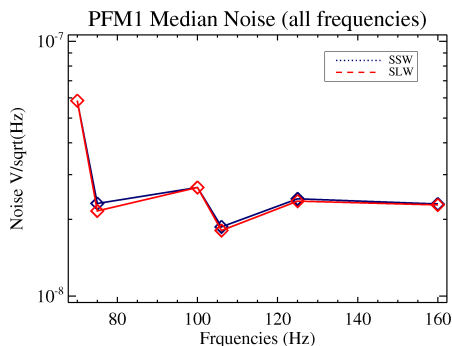


Figure 16: Median array noise depending on bias frequency for the spectrometer arrays.